Discontinuity of cortical gradients reflects sensory impairment

Noam Saadon-Grosman[a,b], Zohar Tal[b], Eyal Itshayek[c], Amir Amedi[b,d], and Shahar Arzy[a,b,1]

[a]Neuropsychiatry Laboratory, Department of Neurology, Hadassah Hebrew University Medical Center, Jerusalem 9112001, Israel; [b]Department of Medical Neurobiology, Faculty of Medicine, The Hebrew University, Jerusalem 9112001, Israel; [c]Department of Neurosurgery, Hadassah Hebrew University Medical Center, Jerusalem 9112001, Israel; and [d]The Edmond and Lily Safra Center for Brain Sciences, The Hebrew University, Jerusalem 9190401, Israel

Edited by Barry E. Stein, Wake Forest University School of Medicine, Winston-Salem, NC, and accepted by the Editorial Board November 13, 2015 (received for review March 29, 2015)

Topographic maps and their continuity constitute a fundamental principle of brain organization. In the somatosensory system, whole-body sensory impairment may be reflected either in cortical signal reduction or disorganization of the somatotopic map, such as disturbed continuity. Here we investigated the role of continuity in pathological states. We studied whole-body cortical representations in response to continuous sensory stimulation under functional MRI (fMRI) in two unique patient populations—patients with cervical sensory Brown-Séquard syndrome (injury to one side of the spinal cord) and patients before and after surgical repair of cervical disk protrusion—enabling us to compare whole-body representations in the same study subjects. We quantified the spatial gradient of cortical activation and evaluated the divergence from a continuous pattern. Gradient continuity was found to be disturbed at the primary somatosensory cortex (S1) and the supplementary motor area (SMA), in both patient populations: contralateral to the disturbed body side in the Brown-Séquard group and before repair in the surgical group, which was further improved after intervention. Results corresponding to the nondisturbed body side and after surgical repair were comparable with control subjects. No difference was found in the fMRI signal power between the different conditions in the two groups, as well as with respect to control subjects. These results suggest that decreased sensation in our patients is related to gradient discontinuity rather than signal reduction. Gradient continuity may be crucial for somatotopic and other topographical organization, and its disruption may characterize pathological processing.

somatotopy | plasticity | whole-body representation | topographic maps | fMRI

The somatotopic "homunculus" representation in the human cortex is one of the most important discoveries of modern neuroscience (1, 2). The early electrophysiological findings of Penfield and coworkers (1, 2) have been confirmed and extended in several neuroimaging studies in healthy individuals (3–7) and have been further explored in patients and nonhuman primates with different pathologies using both electrophysiology and neuroimaging (8–14). The latter elicited changes in the cortical pattern of activity after a damage to the somatosensory system, manifested as functional cortical reorganization. Kaas, Merzenich, and Killackey suggested that there may be "several types of cortical reorganization, including (*i*) the somatotopic expansion of previously existing representations of body parts, (*ii*) the development of 'new' representations, (*iii*) the activation of large regions of the cortex from a very limited region of a receptive field surface, and (*iv*) a 'nonsomatotopic' activation of the cortex from scattered receptive fields" (9). The first three reorganization options were established whereas non-somatotopic representation remains understudied and unclear. A potential explanation is that most previous studies focused on the reorganization of single organ representation or changes in limited cortical area without exploring large scale topographical changes. We hypothesized that large scale nonsomatotopic reorganization may be associated to the relationship between the representation of the disturbed body part and the whole-body representation. In fact, the whole-body representation may have particular importance because continuous somatotopic organization reflects not only adjacency of different body parts, but also the general principle that neural populations that are involved in similar computational tasks are located in close spatial proximity (15, 16). Nonsomatotopic discontinuous whole-body representation may thus reflect a general pathological principle.

To examine the role of continuity and discontinuity in somatosensory processing, we searched for a model that would enable us to compare processing of physiological and pathological whole-body continuous signals in the same study subject. One such model is the cervical partial (sensory) Brown-Séquard syndrome. This syndrome is characterized by injury to one half of the spinal cord, which disturbs sensory signal conduction from half of the body below the lesion to the contralateral hemisphere (17, 18). Patients with Brown-Séquard syndrome experience a reduction in sensation of one side of their body (hemihypoesthesia). Cervical Brown-Séquard syndrome is unique, involving a unilateral representation of the body, but in patients without brain pathology, thus serving as an ideal model to compare physiological and pathological cortical patterns from the disturbed and nondisturbed body sides in each individual patient. Another model that may causally demonstrate the role of continuity and discontinuity in somatosensory processing is one involving patients before and after surgical repair of cervical disk protrusion. This model enables examination of continuity in the

Significance

Topographic organization is a key feature of human brain function, from visual, auditory, and somatosensory processing to numerosity and attention. How is topography affected in pathological states? To unravel this mystery, we scanned whole-body topographic representations under functional MRI in two unique patient populations and quantified continuity and signal power. In patients with sensory Brown-Séquard syndrome, only half of the body is impaired, enabling comparison of disturbed and nondisturbed body sides; in patients undergoing surgical repair, we compared topographies before and after intervention. In each individual patient, pathological processing was reflected by discontinuity of topographic maps rather than signal reduction. These findings highlight the importance of continuity in topographic organization and may serve as a biomarker for somatosensory pathologies.

Author contributions: N.S.-G., Z.T., E.I., A.A., and S.A. designed research; N.S.-G., E.I., and S.A. performed research; N.S.-G. and S.A. contributed new reagents/analytic tools; N.S.-G. and S.A. analyzed data; and N.S.-G., Z.T., E.I., A.A., and S.A. wrote the paper.

The authors declare no conflict of interest.

This article is a PNAS Direct Submission. B.E.S. is a guest editor invited by the Editorial Board.

[1]To whom correspondence should be addressed. Email: shahar.arzy@ekmd.huji.ac.il.

This article contains supporting information online at www.pnas.org/lookup/suppl/doi:10.1073/pnas.1506214112/-/DCSupplemental.

Downloaded at Palestinian Territory, occupied on December 9, 2021

www.manaraa.com

same study subjects before and after intervention. Notably, whereas studies in nonhuman primates compare response to lesion before and after induction, no such study, to our knowledge, has examined response to surgical repair. We therefore used functional MRI (fMRI) in these two patient populations to compare responses in the most prominent somatosensory homunculi—the primary somatosensory cortex (S1) and supplementary motor area (SMA) (1, 19)—with continuous sensory stimulation of the whole body.

To describe a sequential change in cortical activation coinciding with continuous sensory stimulation, we use the term "gradient" (20, 21). We quantified the continuity of gradients by analyzing a one-dimensional series of functional cluster geometric centroids that represent responses to sensory input from different body parts. Signal power was measured as well because somatosensory deficit that results in hypoesthesia may be reflected in signal reduction. We hypothesize that somatotopic representation in the hemisphere contralateral to the sensory deficit exhibits functional reorganization manifested as gradient discontinuity.

Results

Five patients with partial Brown-Séquard syndrome due to disk protrusion, manifested as hemihypoesthesia, and four patients with hypoesthesia due to cervical disk protrusion pending surgical repair (Fig. S1), as well as age-matched healthy controls, were stimulated with a continuous somatosensory stimulation of their right and left body sides under fMRI. We looked for quantitative changes in gradient continuity and signal power between the two hemispheres (in the Brown-Séquard group), before and after surgical repair (in the surgical group) and relative to healthy controls. To characterize somatotopic gradients in the S1 and SMA cortices, we first analyzed the continuous stimulation fMRI data using cross-correlation analysis over 12 different lag-values, corresponding to different body parts sequentially organized from head to toe. This procedure yielded gradient representations of S1 and SMA homunculi in the contralateral hemisphere for the stimulated body side, corroborating previous studies (22, 23) (Fig. 1 and Fig. S2). The exact locations of the gradients were further verified using a block design paradigm (repeated stimulation of cheek, palm, and toes) and a general linear model (GLM) analysis. To objectively quantify gradient continuity, we developed the following analysis. The different lag-values of each gradient were first segmented into clusters (Fig. 2*A*). Geometric centroids were projected on a linear-fit, and lag-values were then organized according to their projection on this fit (Fig. 2*B*). The variance of the difference series was defined as the gradient dispersion value (GDV), characterizing the continuity of the gradient (better continuity is reflected by lower variance and therefore lower GDV) (for details, see *Methods*). To best capture the main axis of the gradient, the linear fit was rotated (±35°) and translated (within four intervals between the extrema of vertical axis components) to obtain minimal GDV (Fig. 2*C*).

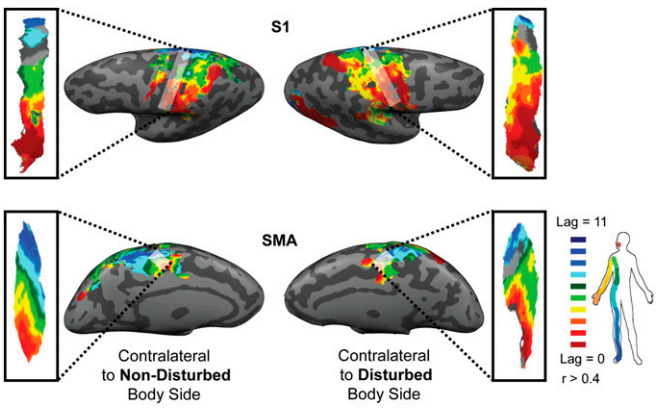

Fig. 1. Qualitative representation of gradients in a representative patient with Brown-Séquard syndrome. Cross-correlation maps corresponding to continuous somatosensory stimulation of a patient with left hemihypoesthesia due to partial cervical Brown-Séquard syndrome are shown. Note the continuous character of gradients in the hemisphere contralateral to the healthy body side in the primary somatosensory cortex (S1; *Upper Left*) and supplementary motor area (SMA; *Lower Left*), compared with discontinuous gradients in the hemisphere corresponding to the disturbed body side (*Right*). Color scale represents body parts from lips (dark red) to toe (dark blue). Extracted gradients (white rectangles) are magnified (for an example of a patient before and after surgical repair, see Fig. S2).

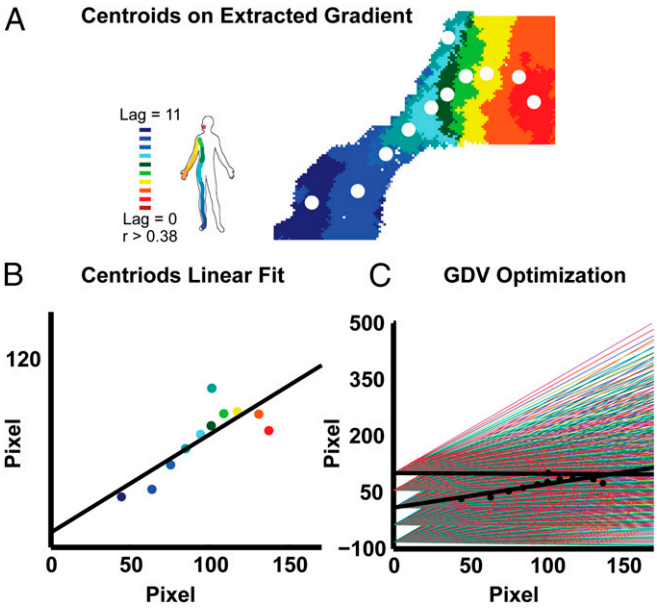

Fig. 2. Gradient quantification. (*A*) The original functional image of a gradient is shown, including centroids corresponding to clusters of different lag-values. (*B*) Centroids are shown with the corresponding lag color and linear fit. (*C*) Trend line optimization: centroids (black) projected on different trend lines (red dots) varying 35 degrees rotation clockwise and anti-clockwise and four vertical translations. Black lines represent the original linear fit and the variation that yielded the lowest gradient dispersion value (GDV).

Brown-Séquard Syndrome Results: Higher GDV Characterizes the Representation of the Disturbed Body Side. Qualitative examination of both S1 and SMA homunculi revealed differences in each individual patient between the contralateral response to the disturbed and to the nondisturbed body side (Fig. 1). This difference is reflected in the topographical pattern when gradients contralateral to the disturbed body side are less continuous. For each individual patient, gradients contralateral to the disturbed body side showed higher GDV than gradients contralateral to the nondisturbed body side, in both the S1 and the SMA (Fig. 3*A* and Table 1). Statistical analysis at the group level confirmed these results (Wilcoxon rank sum, $P < 0.05$). Significant differences were found also when gradients reflecting the disturbed body side were compared with those of control subjects ($P < 0.05$). No difference was found when gradients corresponding to the nondisturbed body side were compared with control subjects, as well as between the right and left sides of the control subjects (all Ps > 0.05) (Fig. 3*A*). These results suggest that hypoesthesia is reflected in a discontinuity of the corresponding somatosensory cortical gradient.

We further inquired whether this disturbance was also reflected in the power of the fMRI signal. For this purpose, we analyzed the percent change of the fMRI blood-oxygen-level

NEUROSCIENCE

Downloaded at Palestinian Territory, occupied on December 9, 2021

www.manaraa.com

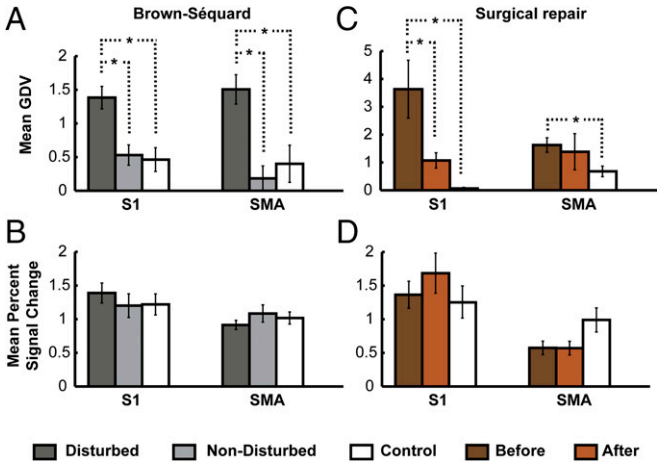

Fig. 3. Group analysis of GDV and signal power. (*A*) Brown-Séquard group: GDV. Mean GDVs of all patients' gradients contralateral to the disturbed (dark gray) and nondisturbed (light gray) body sides, as well as healthy controls (white, averaged over both hemispheres), are presented for S1 (*Left*) and the SMA (*Right*) separately. Note the difference between disturbed and nondisturbed/control gradients ($P < 0.05$), as well as the similarity between nondisturbed gradients and healthy controls. Error bars represent SEM. (*B*) Brown-Séquard group: signal power. Percent signal change of whole-body representation in all conditions did not reveal any significant differences. (*C*) Surgical repair group: GDV. Mean GDVs of all patients' gradients before (dark brown) and after (light brown) surgical repair, as well as healthy controls (white), are presented for S1 (*Left*) and the SMA (*Right*) separately. (*D*) Surgical repair group: signal power. Percent signal change of whole-body representation did not reveal any significant differences between conditions.

dependent (BOLD) signal, averaged separately over the different body parts for S1 and SMA. This analysis did not reveal any significant difference between the disturbed and nondisturbed body sides or between the different sides compared with the healthy controls (all Ps > 0.05) (Fig. 3*B* and Fig. S3).

Surgical Repair Results: Lower GDV Characterizes Whole-Body Representation After Surgical Repair. To further support our results in the Brown-Séquard model, we examined gradient continuity (as reflected in the GDV) and signal power in patients undergoing surgical repair of cervical disk protrusion. Improvement of both GDVs and patients' subjective reports after surgical repair will add more causal support for the role of gradient continuity in somatosensory processing. Qualitative examination of both S1 and SMA homunculi revealed differences between cortical response to sensory stimulation before and after surgery (Fig. S2). Quantitative analysis showed improvement in gradient continuity (lower GDV) after surgical repair in all patients in S1, and in three out of four patients in the SMA (Fig. 3*C* and Table 2). Accordingly, statistical analysis at the group level showed significant difference between the two conditions at S1, and between patients and controls in both S1 and the SMA (Wilcoxon rank sum, $P < 0.05$). Similarly to our findings in patients with Brown-Séquard syndrome, analysis of the percent change in the BOLD signal, averaged separately over the different body parts for S1 and SMA, did not reveal any significant difference before and after surgical repair, as well as between patients and healthy controls (all Ps > 0.05) (Fig. 3*D* and Fig. S4).

Discussion

Functional quantification of the somatosensory gradients in two unique models—patients with partial Brown-Séquard syndrome and patients before and after surgical repair of cervical disk protrusion—revealed several novel findings: For the Brown-Séquard group, gradient continuity was disturbed in the hemisphere contralateral to the disturbed body side at the S1 and SMA cortices, whereas gradients at patients' hemispheres contralateral to the nondisturbed body side were similar to those of healthy controls. For the surgical group, gradient continuity was disturbed before, but not after, surgical repair. Percent signal change of the BOLD signal did not show any significant and consistent power difference in both patient groups.

The underlying pathology in both patient populations involves a disruption of signal conduction from the peripheral sensors to the brain due to spinal cord lesion. In our patients, this disruption led to decreased sensation. Our results relate this disturbance to a discontinuity of cortical gradients rather than signal reduction and stress the central role of gradient continuity in whole-body somatosensory sensation. Gradient discontinuity may further explain nonsomatotopic organization in the context of a whole-body representation.

Reorganization of the homunculi in response to pathologies along the somatosensory pathway has been reported in both animals and humans. Studies in nonhuman primates have reported an expansion of adjacent body parts' representations after spinal cord injuries and amputations (24–28). By using fMRI, similar results were found in human patients with spinal injuries and amputations (29–32). Moreover, it was suggested that perceptual changes go beyond what can be explained by shifts in neighboring cortical representational zones. For instance, fMRI in nonhuman primates after partial section of the dorsal column of the spinal cord at the cervical level showed dispersion of representations of each finger, which were further assembled later (33). Coactivation of nonadjacent representations was found as well, suggesting that cortical reorganization is dispersed over the somatosensory cortex

Table 1. Individual patients and controls data: Brown-Séquard

Subject	Gender	Age	Hypoesthesia	Cord compression	S1 RBS	S1 LBS	SMA RBS	SMA LBS
pBS 1	M	32	R	R	1.329	1.060	1.839	0.923
pBS 2	F	25	L	L	0.447	1.500	0	2
pBS 3	M	50	L	L	0.527	0.809	0	1.571
pBS 4	M	54	L	L	0.491	1.444	0	0.750
pBS 5	M	48	R	R	1.839	0.125	1.374	0
C1	M	24	—	—	0.491	0.410	0	0.238
C2	M	55	—	—	0.544	0.111	0	0
C3	F	50	—	—	0.447	0.111	1.611	1.352
C4	F	28	—	—	0.238	0	0.143	0
C5	F	50	—	—	0.750	1.528	0	0.667

GDVs in S1 and SMA under continuous contralateral stimulation are noted for each individual subject with respect to the clinical disturbance. Notably, for all patients, laterality of cord compression corresponded to the sensory impaired body side. C, control; LBS, left body side; pBS, Brown-Séquard patient; RBS, right body side. —, not applicable.

Downloaded at Palestinian Territory, occupied on December 9, 2021
www.manaraa.com

Table 2. Individual patients and controls data: Surgical repair

Subject	Gender	Age	S1 before	S1 after	SMA before	SMA after
pSR 1	M	37	3.367	0.809	1.6	0.4
pSR 2	M	35	6.222	1.862	2	1.444
pSR 3	F	28	3.789	0.611	2	3.2
pSR 4	F	36	1.151	1	0.9	0.491
C1	M	24	0.125	—	0.982	—
C3	F	50	0	—	0.125	—
C4	F	28	0	—	0.75	—
C5	F	50	0.143	—	0.857	—

GDVs in S1 and SMA under continuous contralateral stimulation are noted for each individual subject before and after surgical repair. Values are noted for the more-disturbed body side. Note the correspondence of subjective report of improvement with improvement of the GDV. C, control; pSR, surgical repair patient. —, not applicable.

(34). Although these studies explained much about somatotopic reorganization, the significance of adjacency is still to be investigated. The pathologies we used here enabled an extension of these findings in humans by comparing whole-body representation in each patient and characterizing reorganization as large scale topographical changes. Moreover, our quantitative analysis pointed out gradient continuity as the feature being modified. Gradients enable computation with respect to neighboring values rather than absolute values. This gradient approach may facilitate computational processes because neighboring units will present similar values (15, 16). Such computations are therefore of importance with respect to whole-body representation. Dorsal column partial lesion in nonhuman primates showed that the extent of cortical plasticity is positively correlated with the severity of the lesion and behavioral deficits. These plastic changes were characterized by shifted, scattered, and weakened BOLD responses at 4 wk postlesion, and then a return and recovery of BOLD responses toward the prelesion state at 8 wk postlesion (35). Such dynamical changes suggest that topographic representations are maintained dynamically, manifesting a self-organizing capacity to restore somatotopic representation (35, 36). Although previous studies investigated mostly hand representation, whole-body representation may better capture such changes and their correlation to behavioral changes and patients' subjective reports.

A unique feature of animal studies is the ability to compare test and retest after lesion induction (11, 13, 24, 28). Here, we suggest a comparable model in humans: patients before and after surgical repair. This model is evidently limited due to chronic changes in patients, quality of repair, or heterogeneity. However, patients reliably report changes in subjective sensation. All our patients reported significant subjective improvement in sensation after surgical intervention, which was further reflected in the GDVs. Further research in a larger cohort of patients may enable the testing of not only a general improvement but also a precise correlation of subjective report and objective measurements of cortical response.

Topographic representations are ubiquitous in the primary cortices: Visual retinotopic maps represent projections of the visual field on the retina; auditory cortex contains tonotopic maps, reflecting the representation of sound frequencies; motor and somatosensory cortices contain homunculus maps corresponding to the representation of body parts (1, 23, 37–39). Recent studies show that topographic organization characterizes not only the primary cortices but also higher order cortices, processing functions such as spatial attention and numerosity (40–43). Gradient continuity may therefore be of importance not only to somatotopic organization but also to topographic organization in general.

The combination of quantitative measurements and neurological pathologies is of much importance for both the scientific study of brain processes as well as clinical implication. Study of unique pathologies such as Brown-Séquard Syndrome (for somatosensory) or nondecussating retinal-fugal fiber syndrome (for vision) (44) presents a most valuable contribution to the neurosciences. In most systems, an early decussation makes distinction of the unilateral external stimulus difficult. These syndromes are therefore a unique model that may distinguish lateralization of the stimuli, enabling comparisons of disrupted and nondisrupted conduction in the same study subjects. Studies in patients undergoing surgical intervention enable experimental examination in lesional and nonlesional states in the same study subject. To be sure, such disorders correspond with most rigorous experimental animal models, yet enable subjective reports of deficits and effects of experimental manipulations in humans. Quantitative measurements of visual, auditory, and somatosensory gradients can be used for in-depth analyses of respective pathologies (45–48), enabling objective evaluation and better understanding of pathological processes and recovery.

Our study included five patients with Brown-Séquard syndrome and four patients undergoing surgical repair of cervical disk protrusion, encompassing all patients with the corresponding pathologies who were treated at our institute over a period of 24 mo and who agreed to participate in the study, met inclusion criteria, and were MRI-compatible. Despite the small number of patients in each group, the ability to compare disturbed and nondisturbed conditions in the same study subject strengthens the results. In particular, differences were found not only at the group level but also in each individual patient. Such patients may further serve as a powerful model to study somatosensory deficits in humans where the subjective experience of sensory deficit is crucial. Brown-Séquard syndrome in our patients was partial, unlike lesion induction in animal models. However, patients reported a significant difference between body sides, as reflected in our results. This study was also confronted with a few other limitations. First, light touch stimulation was conducted manually; however, the protocol was preplanned and the experimenter followed precise stimulus-locked instructions. Moreover, brushing was proved to be superior on other, better-controlled techniques, such as air puff (49), as was also found in our previous experience (22). Second, the substantial variation among different subjects yielded differences in the extracted gradients. To control for these differences, extraction was verified in three anatomical representations (3D, inflate, flattened), including signal evaluation, and was verified by an additional GLM analysis over a standard block design paradigm. Moreover, all potential trend lines to the extracted gradients in a range of ±35 degrees from the linear fit were examined to identify an optimal gradient. Finally, homunculi differ in size; thus, segmentation to clusters with the same lag had various threshold values for minimum pixels per cluster. Nonetheless, the threshold settings were always identical for each individual subject in the compared homunculi (left and right for the Brown-Séquard group, before and after surgery for the surgical repair group). Furthermore, we conducted an additional analysis that did not imply thresholding for all gradients, which yielded similar results (*SI Methods* and Tables S1 and S2).

In conclusion, here, we showed that a sensory deficit due to spinal cord injury is reflected in cortical gradient discontinuity, rather than signal power reduction. We suggest that gradient continuity is a crucial property of brain function and that its disruption is a main character of pathological signal processing. Further research is needed to investigate gradient organization in other sensory modalities, in higher order cortices, as well as the role of gradient organization and its potential disruption in brain pathologies.

Methods

Participants. This prospective cohort study was composed of five patients with hemihypoesthesia (unilateral) related to partial Brown-Séquard syndrome due to cervical disk protrusion [four males, 41.8 ± 11.8 y of age (mean ± SD)],

NEUROSCIENCE

Downloaded at Palestinian Territory, occupied on December 9, 2021
www.manaraa.com

four patients with cervical disk protrusion who underwent surgical repair (two males, 34.0 ± 4.1 y of age), and five age-matched healthy volunteers (two males, 41.4 ± 13.1 y of age). One patient who participated in the Brown-Séquard group and who aggravated 18 mo later was rescanned also before and after surgery. No participant had any other neurological, psychiatric, or systemic disorder. Patients underwent a semistructural interview that documented time of pathology onset, symptoms, and their development, past medical history, and family and social history. Neurological examination elicited normal muscle strength and moderate to severe hypoesthesia for light touch for all patients (for the Brown-Séquard patients: in the affected body side). All patients underwent MRI of the cervical spine, including T1, T2, and short TI inversion recovery (STIR*) contrasts in sagittal and axial views (Fig. S1). All participants gave written informed consent, and the study was approved by the ethics committee of the Hadassah Hebrew University Medical Center.

Stimuli and Procedures. Patients and healthy controls underwent two different stimulation paradigms: continuous (periodic design) and discrete (block design). In the continuous stimulation, a whole-body brush movement was applied lip-to-toe and toe-to-lip bilaterally in two different scanning sessions. Each scanning session contained 14 whole-body stimulation cycles, 7 to each body side. The length of each stimulation cycle was 15 s, which was followed by a 12-s rest baseline. Session started with 30 s of silence before the first cycle onset and ended with 4.5 s after the last cycle offset, in addition to 12 s of silence between body sides.

In the discrete stimulation paradigm, the right and left toes, palm, and cheek were stimulated in separate blocks (yielding six conditions). Each body part stimulation was repeated four times in a randomized order. Stimulation lasted 6 s followed by 9-s rest. Sessions started with 28 s of silence before the first cycle onset and ended with 6 s after the last cycle offset. In concordance with the patient's deficit, in both stimulation paradigms, a natural light-touch stimulation was delivered using a 4-cm-wide paint brush by the same experimenter, who was well-trained before the scans to maintain a constant pace and pressure during the sessions. The experimenter wore fMRI-compatible electrodynamic headphones, which delivered preprogrammed (Presentation; Neurobehavioral Systems) auditory cues signaling the precise timing of the body part sequence, which enabled a controlled velocity of tactile stimuli.

Functional MRI Image Acquisition Procedures and Preprocessing. Patients and controls were scanned at the same site using a Siemens Trio 3T system (32-channel head coil) with the same imaging sequence. Blood oxygen level dependent (BOLD) fMRI was acquired using a whole-brain, gradient-echo (GE) echoplanar (EPI) [repetition time (TR)/time echo (TE) = 1,500/27 ms, flip angle = 70, field of view (FOV) = 192 × 192 mm, matrix = 64 × 64, 26 axial slices, slice thickness/gap = 4 mm/0.8 mm. In addition, high resolution (1 × 1 × 1 mm) T1-weighted anatomical images were acquired to aid spatial normalization to standard atlas space. The anatomic reference volume was acquired along the same orientation as the functional images [TR/TE = 2,300/2.97 ms, matrix = 256 × 256, 160 axial slices, 1-mm slice thickness, inversion time (TI) = 900 ms].

Preprocessing was performed using the Brain Voyager QX 2.8.4.2645 software package (Brain Innovation), including head motion correction, slice scan time correction, and high-pass filtering (cutoff frequency, two cycles per scan). Temporal smoothing (FWHM = 4 s) and spatial smoothing (FWHM = 4 mm) were applied on the periodic design. Functional and anatomical datasets for each subject were aligned and fit to standardized Talairach space (50).

Cross-Correlation Analysis. A boxcar function (3 s) was convolved with a two gamma hemodynamic response function (HRF), to derive a predictor for the analysis. This predictor and the time course of each voxel were cross-correlated, allowing for 12 lags with one TR (time repetition) interval time to account for the stimulation duration of each cycle (10 TRs) and two additional TRs to account for the hemodynamic delay. For each voxel, we obtained the lag-value with the highest correlation coefficient between the time course and 1 of 12 predictors and the value of this correlation coefficient (*SI Methods*).

Gradient Quantification Analysis. The above procedure yielded map values (lag and correlation coefficient), corresponding to vertex coordinates of the brain surface (flat). For patients with Brown-Séquard syndrome, in whom we compared left and right gradients, we chose a correlation threshold that best captured S1 and SMA gradients separately for each subject, constant for both sides (mean, 0.37; SD, 0.035). For patients that underwent surgical repair, in whom we compared gradients before and after surgery, threshold was kept constant for all maps (0.30) (*SI Methods*). Gradients of the primary somatosensory and the supplementary motor cortex were extracted by defining a patch of interest (POI) on the flat cortex surface (*SI Methods*). Each lag and its corresponding coordinates were represented by a specific color in an RGB image matrix. The matrix was segmented into clusters with the same lag-value (Fig. 2*A* and Fig. S5). The cluster-size threshold, set according to the gradient size, defined the minimum number of pixels that accounted for a cluster (*SI Methods*). In a next step, we have calculated the coordinates of a geometric centroid for each cluster. Centroids were plotted on an *x*–*y* plane in which the axes preserved the original image scale. To further define a vector that best represented the quality of the gradient, centroids were projected on a linear fit (Fig. 2*B* and Fig. S5). This manipulation yielded a one-dimensional series of lag-values reflecting the cluster organization and order. Continuity of the gradient was defined with respect to the differences between lags, giving rise to a derivative vector. The gradient was characterized according to the variance of this derivative vector (variation from a "perfectly" organized gradient). This value was thus termed the gradient dispersion value (GDV). To find an optimal fit (lowest GDV), on which centroids were projected, we performed multiple rotations (35 degrees clockwise and counter clockwise, 1-degree step) and translations (within four intervals between the extrema of vertical axis components) of the linear fit which covered the potential line orientation through the scattered centroids (Fig. 2*C*). Corresponding GDVs were calculated while the minimal value was extracted to best capture the gradient's continuity and monotonicity. To test for significant differences between averaged groups of GDVs we used the Wilcoxon rank sum test.

Block Design Analysis. A general linear model (GLM) was applied to the block design data, using predictors (boxcar function, 6 s) convoluted with a two gamma HRF for each of the six conditions (cheek, palm, and toes, bilaterally). Activation maps for each body part were obtained by contrasting each condition versus baseline, to verify the gradient localization. The peak activations for the cheek and toes in the contralateral postcentral gyrus were defined as the start and end point of the S1 homunculus and were compared with the gradient maps obtained from the continuous stimulation. For the SMA homunculi, the localization was verified by the peaks along the medial walls.

Power Analysis. To test whether the disturbance in somatosensory inputs was also reflected in the power of the fMRI signal, we quantified the power of the BOLD signal in each homunculus using the block design data. We extracted a patch of interest (POI) of the contralateral S1 and SMA from the inflated presentation of each contrast (cheek, palm, and toes) containing the most significant 50 and 10 vertices, respectively. This method therefore does not require correction for multiple comparisons because only the most significant vertices are selected. Percent signal change was calculated as the maximum value of epoch-based (−1 to 1 TR around condition onset) event-related averaging.

ACKNOWLEDGMENTS. We thank our patients for their kind agreement to participate in the study; Prof. M. Gomori, Mrs. S. Fisch, Mrs. O. Shamir, Dr. A. Bick, O. Asulin, and the staff of the MRI unit of Hadassah Hebrew University Medical Center for help in patients' management; Prof. M. Timme, M. Peer, Dr. U. Hertz, and S. Aboud for help in data analysis; and Dr. L. Grosman, Prof. T. Ben-Hur, D. Arzi, and R. Shilo for thoughtful discussions and support. This study was supported by a Marie Curie Intra-European Fellowship within the framework of European Union-Seventh Framework Programme for Research and Technological Development PIEFGA-2012-328124 and by the Templeton Foundation within the framework of the Immortality Project, led by Prof. John M. Fischer (S.A.); the Levzion Program (Z.T.); European Research Council Grant 310809; and The James S. McDonnell Foundation Award 220020284 (to A.A.).

1. Penfield W, Boldrey E (1937) Somatic motor and sensory representation in the cerebral cortex of man as studied by electrical stimulation. *J Neurol* 60: 389–443.
2. Penfield W, Rasmussen T (1950) *The Cerebral Cortex of Man: A Clinical Study of Localization of Function* (Hafner, New York).
3. Fox PT, Burton H, Raichle ME (1987) Mapping human somatosensory cortex with positron emission tomography. *J Neurosurg* 67(1):34–43.
4. Nakamura A, et al. (1998) Somatosensory homunculus as drawn by MEG. *Neuroimage* 7(4 Pt 1):377–386.
5. Narici L, et al. (1991) Neuromagnetic somatosensory homunculus: A non-invasive approach in humans. *Neurosci Lett* 121(1-2):51–54.
6. Stippich C, et al. (1999) Somatotopic mapping of the human primary somatosensory cortex by fully automated tactile stimulation using functional magnetic resonance imaging. *Neurosci Lett* 277(1):25–28.

Downloaded at Palestinian Territory, occupied on December 9, 2021
www.manaraa.com

7. Yang TT, Gallen CC, Schwartz BJ, Bloom FE (1993) Noninvasive somatosensory homunculus mapping in humans by using a large-array biomagnetometer. *Proc Natl Acad Sci USA* 90(7):3098–3102.
8. Pons TP, et al. (1991) Massive cortical reorganization after sensory deafferentation in adult macaques. *Science* 252(5014):1857–1860.
9. Kaas JH, Merzenich MM, Killackey HP (1983) The reorganization of somatosensory cortex following peripheral nerve damage in adult and developing mammals. *Annu Rev Neurosci* 6:325–356.
10. Kaas JH (1991) Plasticity of sensory and motor maps in adult mammals. *Annu Rev Neurosci* 14:137–167.
11. Kaas JH (2000) The reorganization of somatosensory and motor cortex after peripheral nerve or spinal cord injury in primates. *Prog Brain Res* 128:173–179.
12. Kaas JH, et al. (2008) Cortical and subcortical plasticity in the brains of humans, primates, and rats after damage to sensory afferents in the dorsal columns of the spinal cord. *Exp Neurol* 209(2):407–416.
13. Nardone R, et al. (2013) Functional brain reorganization after spinal cord injury: Systematic review of animal and human studies. *Brain Res* 1504:58–73.
14. Wall JT, Xu J, Wang X (2002) Human brain plasticity: An emerging view of the multiple substrates and mechanisms that cause cortical changes and related sensory dysfunctions after injuries of sensory inputs from the body. *Brain Res Brain Res Rev* 39(2-3):181–215.
15. Kaas JH (1997) Topographic maps are fundamental to sensory processing. *Brain Res Bull* 44(2):107–112.
16. Silver MA, Kastner S (2009) Topographic maps in human frontal and parietal cortex. *Trends Cogn Sci* 13(11):488–495.
17. Kobayashi N, Asamoto S, Doi H, Sugiyama H (2003) Brown-Sèquard syndrome produced by cervical disc herniation: Report of two cases and review of the literature. *Spine J* 3(6):530–533.
18. Tattersall R, Turner B (2000) Brown-Séquard and his syndrome. *Lancet* 356(9223): 61–63.
19. Penfield W, Jasper H (1954) *Epilepsy and the Functional Anatomy of the Human Brain* (Churchill, London).
20. Goldberg E (1989) Gradiental approach to neocortical functional organization. *J Clin Exp Neuropsychol* 11(4):489–517.
21. Sereno MI, McDonald CT, Allman JM (1994) Analysis of retinotopic maps in extrastriate cortex. *Cereb Cortex* 4(6):601–620.
22. Geva R (2012) Neural correlates of the intrinsic and extrinsic components of the body scheme using fMRI in humans. PhD dissertation (The Hebrew University, Jerusalem).
23. Zeharia N, Hertz U, Flash T, Amedi A (2012) Negative blood oxygenation level dependent homunculus and somatotopic information in primary motor cortex and supplementary motor area. *Proc Natl Acad Sci USA* 109(45):18565–18570.
24. Dutta A, Kambi N, Raghunathan P, Khushu S, Jain N (2014) Large-scale reorganization of the somatosensory cortex of adult macaque monkeys revealed by fMRI. *Brain Struct Funct* 219(4):1305–1320.
25. Florence SL, Kaas JH (1995) Large-scale reorganization at multiple levels of the somatosensory pathway follows therapeutic amputation of the hand in monkeys. *J Neurosci* 15(12):8083–8095.
26. Jain N, Qi H-X, Collins CE, Kaas JH (2008) Large-scale reorganization in the somatosensory cortex and thalamus after sensory loss in macaque monkeys. *J Neurosci* 28(43):11042–11060.
27. Merzenich MM, et al. (1984) Somatosensory cortical map changes following digit amputation in adult monkeys. *J Comp Neurol* 224(4):591–605.
28. Tandon S, Kambi N, Lazar L, Mohammed H, Jain N (2009) Large-scale expansion of the face representation in somatosensory areas of the lateral sulcus after spinal cord injuries in monkeys. *J Neurosci* 29(38):12009–12019.
29. Corbetta M, et al. (2002) Functional reorganization and stability of somatosensory-motor cortical topography in a tetraplegic subject with late recovery. *Proc Natl Acad Sci USA* 99(26):17066–17071.
30. Flor H, et al. (1995) Phantom-limb pain as a perceptual correlate of cortical reorganization following arm amputation. *Nature* 375(6531):482–484.
31. Henderson LA, Gustin SM, Macey PM, Wrigley PJ, Siddall PJ (2011) Functional reorganization of the brain in humans following spinal cord injury: Evidence for underlying changes in cortical anatomy. *J Neurosci* 31(7):2630–2637.
32. Simões EL, et al. (2012) Functional expansion of sensorimotor representation and structural reorganization of callosal connections in lower limb amputees. *J Neurosci* 32(9):3211–3220.
33. Chen LM, Qi H-X, Kaas JH (2012) Dynamic reorganization of digit representations in somatosensory cortex of nonhuman primates after spinal cord injury. *J Neurosci* 32(42):14649–14663.
34. Moore CI, et al. (2000) Referred phantom sensations and cortical reorganization after spinal cord injury in humans. *Proc Natl Acad Sci USA* 97(26):14703–14708.
35. Fang P-C, Jain N, Kaas JH (2002) Few intrinsic connections cross the hand-face border of area 3b of New World monkeys. *J Comp Neurol* 454(3):310–319.
36. Merzenich MM, et al. (1983) Topographic reorganization of somatosensory cortical areas 3b and 1 in adult monkeys following restricted deafferentation. *Neuroscience* 8(1):33–55.
37. Engel SA, et al. (1994) fMRI of human visual cortex. *Nature* 369(6481):525.
38. Lauter JL, Herscovitch P, Formby C, Raichle ME (1985) Tonotopic organization in human auditory cortex revealed by positron emission tomography. *Hear Res* 20(3): 199–205.
39. Wandell BA (1999) Computational neuroimaging of human visual cortex. *Annu Rev Neurosci* 22:145–173.
40. Hagler DJ, Jr, Sereno MI (2006) Spatial maps in frontal and prefrontal cortex. *Neuroimage* 29(2):567–577.
41. Harvey BM, Klein BP, Petridou N, Dumoulin SO (2013) Topographic representation of numerosity in the human parietal cortex. *Science* 341(6150):1123–1126.
42. Kastner S, et al. (2007) Topographic maps in human frontal cortex revealed in memory-guided saccade and spatial working-memory tasks. *J Neurophysiol* 97(5): 3494–3507.
43. Silver MA, Ress D, Heeger DJ (2005) Topographic maps of visual spatial attention in human parietal cortex. *J Neurophysiol* 94(2):1358–1371.
44. Victor JD, et al. (2000) Visual function and brain organization in non-decussating retinal-fugal fibre syndrome. *Cereb Cortex* 10(1):2–22.
45. Barnes GR, Hess RF, Dumoulin SO, Achtman RL, Pike GB (2001) The cortical deficit in humans with strabismic amblyopia. *J Physiol* 533(Pt 1):281–297.
46. Baseler HA, Morland AB, Wandell BA (1999) Topographic organization of human visual areas in the absence of input from primary cortex. *J Neurosci* 19(7):2619–2627.
47. Baseler HA, et al. (2002) Reorganization of human cortical maps caused by inherited photoreceptor abnormalities. *Nat Neurosci* 5(4):364–370.
48. Morland AB, Baseler HA, Hoffmann MB, Sharpe LT, Wandell BA (2001) Abnormal retinotopic representations in human visual cortex revealed by fMRI. *Acta Psychol (Amst)* 107(1-3):229–247.
49. Huang R-S, Chen CF, Tran AT, Holstein KL, Sereno MI (2012) Mapping multisensory parietal face and body areas in humans. *Proc Natl Acad Sci USA* 109(44):18114–18119.
50. Talairach J, Tournoux P (1988) *Co-Planar Stereotaxic Atlas of the Human Brain. 3-Dimensional Proportional System: An Approach to Cerebral Imaging* (Thieme, New York).

Downloaded at Palestinian Territory, occupied on December 9, 2021

www.manaraa.com